OPPD

Omaha Public Power District
444 South 16th Street Mall
Omaha, Nebraska 68102-2247
402/636-2000

May 20, 1991
LIC-91-163R

U. S. Nuclear Regulatory Commission
Attn: Document Control Desk
Mail Station P1-137
Washington, DC 20555

References:
1. Conference call from OPPD to NRC, April 23, 1991
2. Letter from NRC (W. C. Walker) to OPPD (W. G. Gates) dated May 2, 1991

Gentlemen:

SUBJECT: Implementation of the Station Blackout Rule, 10 CFR 50.63

This letter transmits Omaha Public Power District's (OPPD) attached responses on the implementation of the Station Blackout Rule in accordance with your Reference 2 request and the additional requests made during the Reference 1 conference call.

If you should have any questions, please call me.

Sincerely,

W. G. Gates

W. G. Gates
Division Manager
Nuclear Operations

WGG/sel

Attachment

c: LeBoeuf, Lamb, Leiby & MacRae
R. D. Martin, NRC Regional Administrator, Region IV
W. C. Walker, NRC Project Manager
R. P. Mullikin, NRC Senior Resident Inspector

A050

RESPONSE TO NRC QUESTIONS ON FORT CALHOUN STATION SBO SUBMITTAL

Q.1. PROPOSED STATION BLACKOUT DURATION

- Application of the criteria of NUMARC 87-00 results in Fort Calhoun being placed in SW and ESW Group "3", while the submittal identifies FCS as category "2" in these areas. Explain this discrepancy.

- *Identify the main disconnect switch "DS-T1" DC power supply source. Verify backfeed from 345KV system can be established within one hour.

RESPONSE

The USAR, NUMARC 87-00, Reg. Guide 1.155, and/or site specific weather data from The National Bureau of Standards Science Series 118, Extreme Wind Speeds at 129 Stations in Contiguous United States were used to identify both SW & ESW categories as follows:

- The estimated frequency of loss of offsite power due to severe weather "SW" Group was determined using Table 6 of Reg. Guide 1.155. The frequency "f" was determined by the following equation:

$$f = (1.3 \times 10^{-4})h_1 + (b)h_2 + (0.012)h_3 + (c)h_4$$

where h_1 = Annual expected snowfall for FCS, in inches
= 30.9 inches (USAR section 2.5.1) -NUMARC Table 3-3 says 29 inches

h_2 = Annual expectation of Tornadoes (winds > 113mph)
= 0.000141 (NUMARC Table 3-3)

b = 12.5 for sites with transmission Lines on two or more Rights of Way, Spreading out in Different directions from the switchyard.

or,

= 72.3 for sites with transmission Lines on one right of way.

From USAR Figure 8.2-2 and DWG A 934, the transmission lines come into FCS from different directions and on several right of ways. Therefore, b = 12.5

h_3 = Annual expectation of storms at FCS with velocities between 75 and 124 mph

NUMARC Table 3-3 says h_3 = 0.5 for FCS. Site specific "Omaha" weather data obtained from the NBS Building Science Series 118 published in March, 1979 by the U.S. Department of Commerce (page 162) predicts a return period of 20 years for 10 meter wind speeds exceeding 75 mph (type I distribution) which correlates to an expected frequency of the h_3 = 1/20 = 0.05 therefore, 0.05 was used in the calculation for h_3. NUMARC table 3-3 could be in error.

h_4 = Annual expectation of hurricanes, does not apply to FCS.

therefore,

$$f = (1.3\times10^{-4})(30.9)+(12.5)(1.41\times10^{-4})+(0.012)(0.05) + 0$$

$$= 6.4 \times 10^{-3}$$

from Table 6 of Reg. Guide 1.155 for $f = 6.4 \times 10^{-3}$

<u>SW = 2</u>

To calculate the h_3 using wind speed of 75mph at 30 meter height, the following conversion equation was used to calculate the equivalent wind speed at 10 meter height:

NBS equation 2.4.6;

$$\frac{U_{fm}(10)}{U_{fm}(Z)} = \frac{U(10)}{U(Z)} \left(1 + \frac{Z - 10}{10} 0.02\right)$$

Where Z = 30 meters
$U_{fm}(10)$ = Fastest wind at 10 meters above ground
$U_{fm}(Z)$ = Fastest wind at 30 meters above ground

$$\frac{U_{(10)}}{U_{(30)}} = \frac{(10)1/7}{30} = 0.85475 \text{ (from Equation 2.4.2)}$$

Plugging the results in Equation 2.4.6

$$\frac{U_{fm}(10)}{U_{fm}(30)} = 0.85475 \left(1 + \frac{30 - 10}{10} 0.02\right)$$

$$= 0.8889$$

Therefore, $U_{fm}(10) = 0.8889\ (U_{fm}(30))$
$= 0.8889$ (75mph)
= 66.7mph

The return period for winds of 75mph at 30 meters is equal to the return period for 66.7mph wind at 10 meters.

From NBS page 162, the return period for winds of 66.7mph at 10 meters above ground is approximately once every seven years or

$$h_3 = 1/7 = 0.142$$

Therefore, $f = (1.3 \times 10^{-4})(30.9) + (12.5)(1.41 \times 10^{-4}) + (0.012)(0.142) + 0$
$= 7.52 \times 10^{-3}$

from Table 6 of Reg. Guide 1.155 for $f = 7.52 \times 10^{-3}$

SW = 2

(Note: 30 Meters above ground is used because it provides more appropriate representation of transmission lines height. It is also more conservative for the h_3 and ESW evaluation.)

- The Extremely Severe Weather (ESW) Group was determined using table 8 of Reg. Guide 1.155. The annual expectation of storms with wind speeds $\geq$ 125 mph at FCS = e. Again The NBS Building Science Series 118 was used to calculate "e". The NBS provides wind data for Omaha at 10 meters above ground. Equations 2.4.2 and 2.4.6 from NBS Building Science Series 118 were used to determine the equivalent wind speeds at 10 meters as follows:

$$U_{fm}(10) = 0.8889\,(U_{fm}(30)) = 0.8889\,(125\text{mph}) = 111.1\text{mph}$$

The return period for winds of 125 mph at 30 meters is equal to the return period for 111.1 mph winds at 10 meters. From NBS Building Science Series 118 page 162, the return period for winds of 111.1 mph at 10 meters above ground is between 1000 and 2000 years (Type 1 Distribution).

Therefore: $1/2000 < e < 1/1000$

$$5 \times 10^{-4} < e < 1.0 \times 10^{-3}$$

from Table 8 of Reg. Guide 1.155, for $5 \times 10^{-4} < e < 1.0 \times 10^{-3}$,

ESW = 2

The additional wind data provided by Mr. Emil Simiu of NBS (attachment 2) does not affect the outcome of the above calculations. The additional data is for the years 1978 through 1986, and should be added to page 161 of NBS Series 118. This additional data will make the return period tabulated on page 162 greater for most extreme wind speeds, specifically for wind speeds 75mph and above.

- The main disconnect "DS-T1" is DC motor operated, with opening time of twenty-four seconds maximum following an initiating signal (Ref. USAR Section 8.2.2). The DC power supply to the switch operating mechanism is provided from The Station 1E batteries, panel "DC-PNL-1". This switch can be opened or closed, as desired, remotely from CB-20, or locally from the panel located near the switch, also the switch can be manually cranked open or closed, provided the prerequisites have been met (Operating Instruction

Procedure OI-EG-1). According to the Operator's experience of transferring loads during refueling outages, back feed from the 345KV system can be accomplished in less than one hour, the Station Blackout "EOP-07" and/or Operating Instruction Procedure "OI-EE-1," depending on the plant condition, provide the required instruction to the operators for backfeeding from the 345KV system.

Attachments:
1. NBS Building Science Series 118, cover page plus pages 1 through 15, 19, 160, 161 and 162.
2. Record of telephone conversation between Mike Elzway (OPPD) and Mr. Emil Simiu of NBS.
3. OPPD Drawing A934.

Q2. BATTERY CALCULATIONS

- What loads will be stripped from the batteries to meet the required 4 hours coping in response to a SBO?
- Will one full division of instrument and control be available, as required by guidance?
- *Provide discussion of the methodology used in the calculation and deviations (if any) from IEEE standards and correction factors used.
- *Provide times of Load Shedding.

RESPONSE

Loads will be stripped in accordance with SBO Procedure EOP-07 as follows:

Battery #1

- Emergency Lighting Panel "ELP1", within 15 minutes
- Turbine Bldg. Emergency Lighting Panel "ELP5", within 15 minutes
- DC Emergency Lube oil pump, within 30 minutes
- Non-safety related Panel AI-42A except for breaker feeding AI-53 (Communication Panel), within 120 minutes

Battery #2

- Aux. Building Vent Room Emergency Lighting Panel "ELP2", within 15 minutes
- 400HZ Inverter, within 15 minutes
- DC Emergency Seal Oil Pump, within 120 minutes

- Non-Safety related panel AI-42B except for breaker feeding AI-53 (Communication Panel), within 120 minutes

Since the Safety Related Invertors A, B, C & D will not be load shed, at least one full division of instrument and control will be available as required by guidance.

- The following is a brief summary of the IEEE 485 methodology used in the battery capacity calculation. There were no deviations from the recommended IEEE methodology other than the assumed aging factor which is discussed below.

  The cell size determination was calculated in accordance with IEEE 485-1983. To verify cell size, it is necessary to calculate, from an analysis of each section of the dc load profile, the maximum capacity required by the combined load demands of the various sections.

  Once the required cell size has been calculated for each section (IEEE 485, Equation 1), the largest cell size is selected and the cell size for random loads added to determine the uncorrected cell size. The random load cell size is also calculated by the same formula.

  The corrected cell size is calculated by correcting the uncorrected cell size for Temperature, Design Margin and Aging. The temperature correction factor is 1.04 (for 70°F), and the Design Margin is 10% (1.10). No correction for Aging is included (the aging factor is 1.00), since the station batteries are tested periodically as required by NRC Regulatory Guide 1.32, IEEE 450-1980, and Fort Calhoun Technical Specifications. Any battery degradation due to aging will be found during periodic testing.

  The batteries are fully charged at the beginning of the SBO Incident and the electrolyte specific gravity is 1.215. Electrolyte temperature does not decline below 70°F during the event.

  DC power required to operate circuit breakers and start the emergency diesel generators to end the SBO event were included in the calculation. A minimum of five (5) diesel starts were included. Also transient loads were included for the 4160 and 480V trip coils, main generator field trip coils and 86 lockout relays. A total of 74 relays for alarms (other than annunciators) are assumed on; these alarms are not required for SBO event.

Q3. <u>LOSS OF HVAC</u>

Explain the following:

- The way in which areas of concern were chosen.
- The initial temperature assumptions.

- *Provide brief discussion of methodology used.
- *Verify that LOCA/MSLB profiles bound the SBO conditions.
- *Justify that the control room initial temperature of 78°F used in the calculation is acceptable.

RESPONSE

The purpose of the room heat-up calculation is to evaluate the effect of loss of HVAC in areas containing equipment necessary to mitigate the consequences of a station blackout. The three main objectives are:

1. Demonstrate the operability of the equipment under the conditions of increasing (or decreasing) temperature due to loss of HVAC.
2. Evaluate the habitability of vital plant areas such as the control room for monitoring and/or manual action purposes.
3. Investigate the likelihood of inadvertent actuation of fire protection systems due to elevated room temperatures.

The rooms which were evaluated for the effect of loss of HVAC were determined by reviewing the location of the equipment required for station blackout. Rooms serviced by HVAC that contain SBO equipment and have heat source(s) were selected for evaluation. The battery rooms were also included since they are serviced by HVAC and the battery capacity can be affected by decreasing temperatures. This selection identified four areas. They are:

AFW Pump Room (Room 19)
Switchgear Area (Rooms 56, 56E)
Control Room (Room 77)
Battery Rooms (Rooms 54, 55)

Containment was excluded from this evaluation since station blackout equipment inside containment is covered under the environmental EQ program and LOCA/MSLB conditions have been verified to envelop the station blackout conditions. The AFW pump room, switchgear rooms and the control room were evaluated for temperature rise effects. The battery rooms were evaluated for temperature drop effects because the battery capacity decreases with decreasing temperature.

The heat transfer calculations were performed using a proprietary computer program. The program accounts for internal heat sources (electrical or hot pipes), heat loss or gain through external walls, and ventilation due to forced or natural circulation. The input data to the program consists of a description of:

Room size and initial temperature
Internal heat sources
External walls
Boundary conditions

The heat transfer models were based on the following conservative assumptions:

1. Normally closed doors at the onset of station blackout remain closed and leak proof throughout the four hour duration. This is a conservative assumption which maximizes the change in room temperatures due to lack of ventilation.

2. Exterior temperatures are at the extreme temperatures given in USAR.

3. For rooms which the concern is elevated temperatures, initial conditions are at maximum summer HVAC design temperatures. These initial conditions are as follows:

AFW Pump room	105°F
Switchgear rooms	105°F
Control room	78°F

For the battery rooms, initial conditions are at 72°F.

The analyses were performed by executing the room models for the duration of station blackout (4 hours). The results show that the temperature in the switchgear rooms, control room and auxiliary feedwater pump does not rise above 112°F. This temperature is significantly lower than the equipment operability limits defined in Appendix F of NUMARC 87-00. The lower limit of operability for the most limiting equipment is set at 160°F in NUMARC 87-00. The calculated temperatures also meet "Condition 1" of Section 2.7 of NUMARC 87-00. "Condition 1" rooms are described as rooms with temperatures less than 120°F. Equipment located in a "Condition 1" environment is considered to be of low concern and does not require special actions to assure operability. In conclusion, operability of station blackout equipment at Fort Calhoun Station is not compromised.

The battery room temperature is 69.6°F. This temperature is only 0.4°F below the 70°F limit used in the battery capacity calculation. This difference is not expected to affect the capacity of the batteries. In reality, the battery temperature will stay above the room temperature due to internal battery losses. This effect has not been considered in this calculation.

The calculation correctly used 78°F, which is the design basis temperature for the control room HVAC units. There are redundant CQE trains of HVAC for the control room, and, therefore, air conditioning is credited prior to SBO. The SBO event is assumed to take out both trains resulting in loss of HVAC for the control room. Control room temperatures would increase above 78°F due to heat loads from electrical equipment (powered by the station batteries), operators, and residual heat. The upper limit on this temperature rise is the 105°F technical specification limit. The control room limit is based on maintaining in-cabinet ambient temperatures to ≤ the electrical equipment qualification temperature of 122°F. The SBO calculation derives the maximum control room temperatures resulting from loss of HVAC for the duration of SBO. This maximum temperature stays below 105°F. This is below the comfort limit of 110°F recommended in Section 2.7.2, Paragraph (3), of NUMARC 87-00. Accordingly, the control room habitability is not affected.

Q4. REACTOR COOLANT INVENTORY

- What primary system RCP leak rate was assumed?
- What are the conditions of the reactor coolant system at the end of the SBO event?
- What was the leak rate calculated for the CEDM seals?

RESPONSE

See attachment #4.

Q5. *CONTAINMENT ISOLATION

- *Isolation valves that do not meet Reg. Guide 1.155 exclusion criteria should be identified and listed in the EOPs for operator's action if plant conditions require containment isolation.

RESPONSE

OPPD, in April 27, 1989, submittal (LIC-89-331) committed to revise procedures to address containment spray and safety injection headers isolation. Containment isolation issue was further reviewed in accordance with Reg. Guide 1.155 exclusion criteria. The results of this review have indicated that a credit can be taken for check valves inside containment on spray headers and both safety injection headers to provide the required isolation if plant conditions warrant containment isolation during station blackout. The check valves inside containment on the safety injection headers are leak rate tested at least once every refueling to satisfy Technical Specification 2.1.1.1(12) requirements. A sample disassembly and inspection surveillance test is performed on one of the spray header check valves every refueling outage. This test satisfies, in part, the requirements of Technical Specification Section 3.3(1)a.

Containment sump recirculation isolation valves are normally closed during plant operation. Since these valves are normally closed, the only potential for being outside Reg. 1.155 guidelines is during quarterly surveillance testing. If station blackout occurs during the testing of these valves, the operator responsible for timing the valve stroke during the test (these valves are tested one at a time) will know the valve position and can take appropriate action to manually close the valve.

It is OPPD's position that the intent of Reg. Guide 1.155 with respect to isolation and position indication has been met. Therefore, procedure revisions committed to in LIC-89-331 are no longer required.

*** Information marked with an asterisk was requested by the NRC during the conference call held between the NRC and OPPD on April 23, 1991.**

ATTACHMENT #1

NBS BUILDING SCIENCE SERIES 118

Extreme Wind Speeds at 129 Stations in the Contiguous United States

Emil Simiu

Center for Building Technology
National Engineering Laboratory
National Bureau of Standards
Washington, D.C. 20234

Michael J. Changery

Environmental Data Information Service
National Climatic Center
National Oceanic and Atmospheric Administration
Asheville, North Carolina 28801

James J. Filliben

Center for Applied Mathematics
National Engineering Laboratory
National Bureau of Standards
Washington, D.C. 20234

Sponsored by:
National Science Foundation
Washington, D.C. 20550 and
Department of Energy
Office of Assistant Secretary,
Conservation and Solar Applications
Washington, D.C. 20545

U.S. DEPARTMENT OF COMMERCE, Juanita M. Kreps, Secretary
Jordan J. Baruch, Assistant Secretary for Science and Technology
NATIONAL BUREAU OF STANDARDS, Ernest Ambler, Director

Issued March 1979

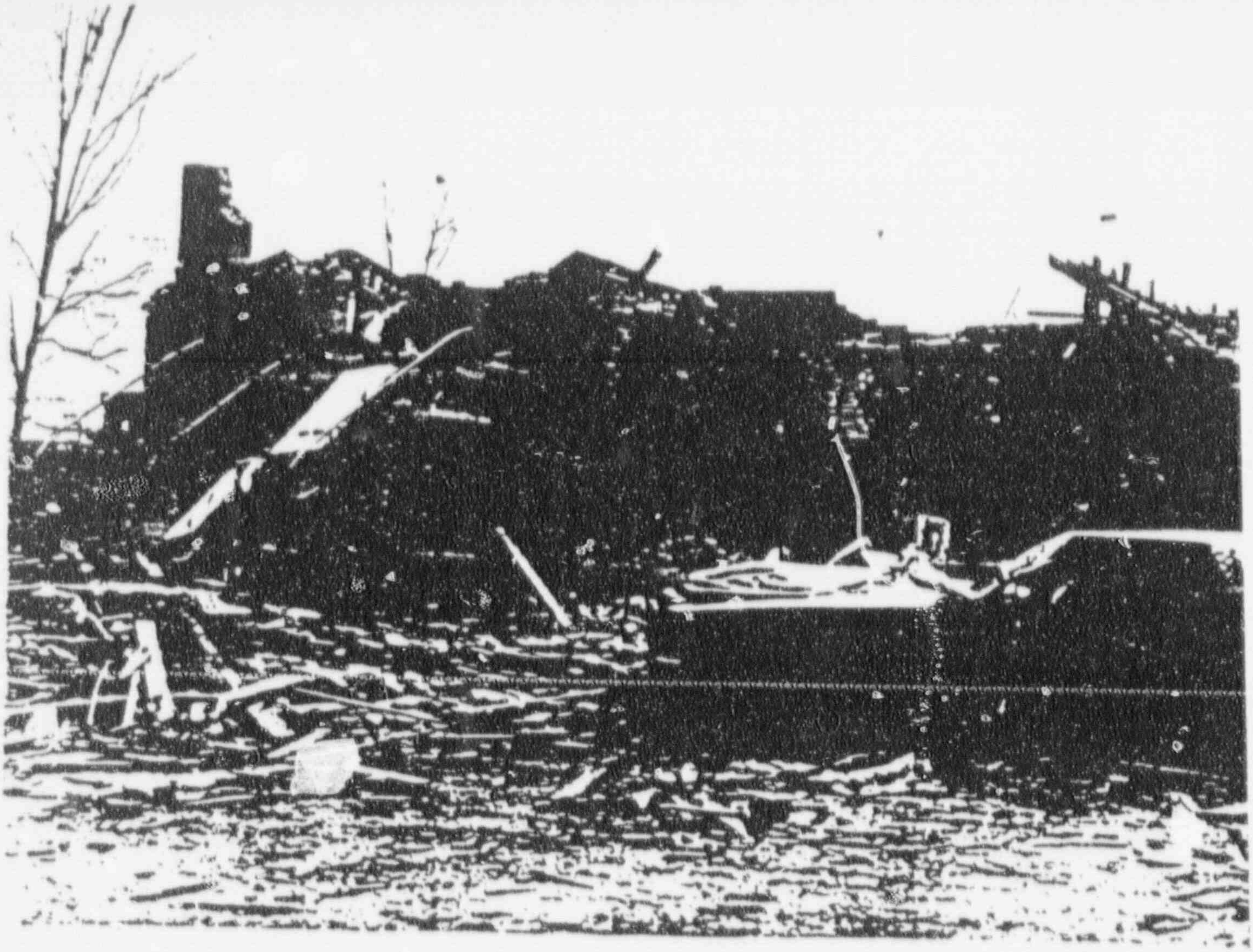

1. INTRODUCTION

The purpose of this report is to present information on extreme wind speeds at 129 airport stations in the contiguous United States at which reliable wind records are available over a number of consecutive years.

This information consists of:

1. Extreme yearly wind speeds, and the corresponding wind directions, recorded at each of the 129 stations. These data were obtained by the National Climatic Center from the original records. Thus, reading errors of original records and errors of transcription that have been determined to be present in Local Climatological Data (LCD) monthly and annual summaries* have been eliminated. The vast majority of the

* A list of stations for which LCD summaries are available can be obtained from the National Climatic Center, Asheville, N.C. 28801. Summaries may be ordered from the Superintendent of Documents, U.S. Government Printing Office, Washington, D.C. 20402.

originally recorded data consisted of fastest-mile speeds. These have been listed without modification in the report. However, at a few stations, some of the recorded data consisted of fastest observed one-minute speeds. These have been transformed into fastest-mile speeds using a relation given in Section 2.1. It is these fastest-mile speeds that have been listed in the report in lieu of the orginally recorded fastest observed one-minute data. The stations and dates at which fastest-minute speeds were originally recorded are listed in Section 2.1.

A few of the wind speed data used herein represent estimates, rather than results of measurement. These data are identified in Section 2.2.

2. Anemometer elevations at which the largest yearly wind speeds were recorded.

3. Largest yearly wind speeds reduced to an elevation of 10m above ground (corrected speeds). These were obtained by using an expression given in Section 2.4.

4. Results of the statistical analysis of the corrected wind speed data. These results include:

- For each of the 129 sets of data, the predicted wind speeds corresponding to various return periods, based on the assumption that the Type I probability distribution of the largest values is a valid description of the extreme wind speeds
- for those sets of data that are best fit by a Type II probability distribution of the largest values, the predicted wind speeds corresponding to various return periods, based on that distribution
- estimates of the lower bound of the standard deviation of the errors inherent in the predicted speeds
- estimates (obtained by the method of moments) of the standard deviation of the errors inherent in the predicted speeds

Extreme wind speed predictions have been included for mean recurrence intervals of up to 1,000,000 years. However, in the writers' opinion, physical considerations suggest that predictions corresponding to mean recurrence intervals beyond a few hundred years should be regarded with caution.

A brief description of the procedure used in the analysis of the data is presented in Section 3. Section 3 includes a summary, and Sections 3.3 and 3.4 a discussion of the results of the statistical analysis. The information described under items 1 through 4 above is included in Section 4 of the report.

It is noted that at a number of stations the extreme yearly wind speed data may not provide a reliable basis for predicting extreme speeds. The results of the statistical analysis for these stations should therefore be regarded with caution. Stations for which such caution is in order are listed in Appendix 1.

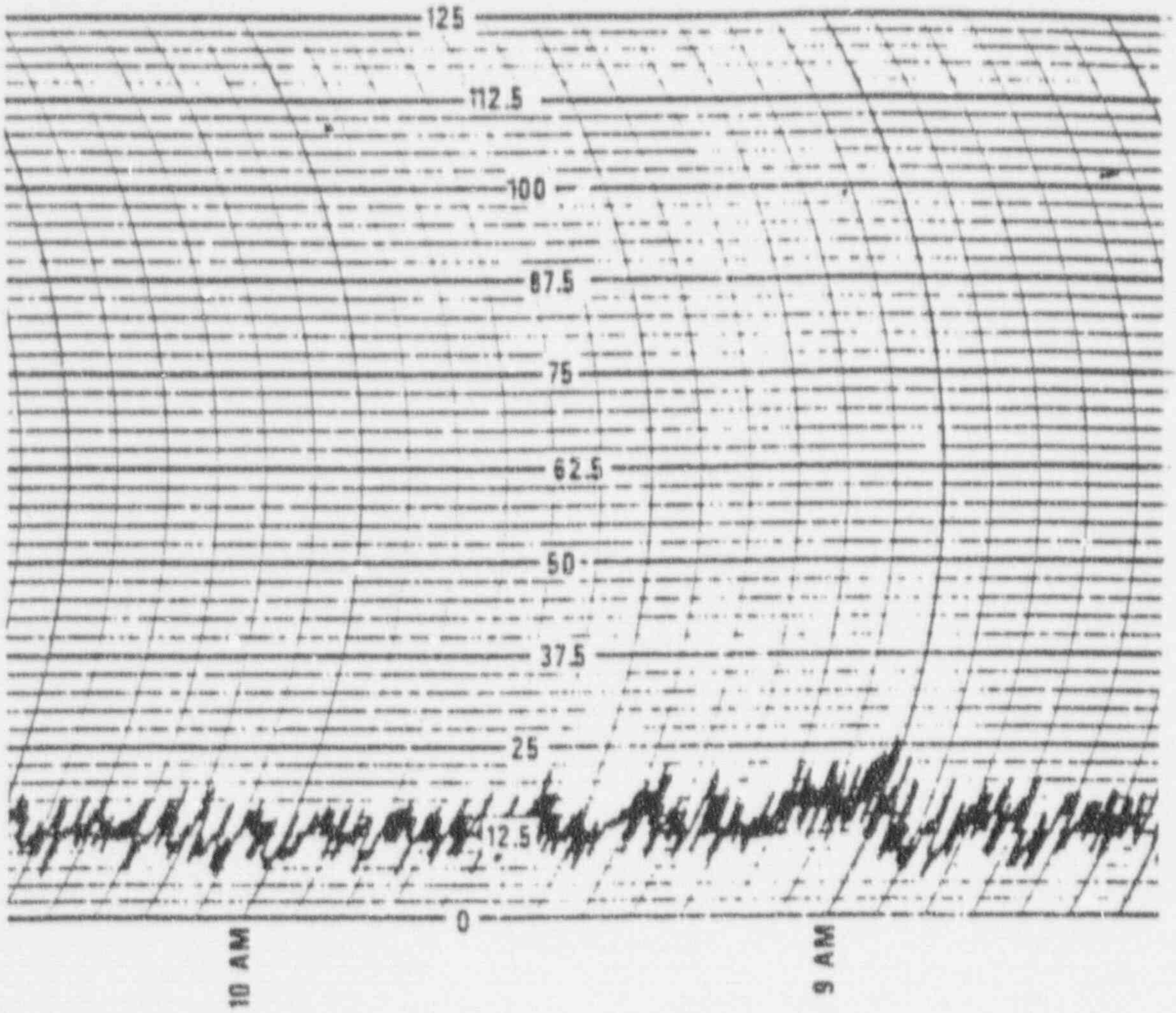

2. WIND SPEED DATA

2.1 FASTEST OBSERVED ONE-MINUTE WIND SPEEDS

It was indicated in Section 1 that the vast majority of the original data used in this report consisted of fastest-mile wind speeds, i.e., speeds averaged over a time interval (in seconds) $t = 3600/v_f$, and v_f = the fastest-mile wind speed in miles per hour. However, at the following stations the original recorded maximum annual wind speed data consisted of fastest observed one-minute speeds during the periods indicated below:

Atlanta, Georgia	(1961 through 1963)
Indianapolis, Indiana	(1962-1963)
Boston, Massachusetts	(1954 through 1958)
Lansing, Michigan	(1955 through 1958)
Sault Ste Marie, Michigan	(1956 through 1965)

According to Reference 1, studies of the relationship between fastest observed one-minute to fastest-mile wind speeds undertaken at four weather stations "showed the mean regression between the two types of observation to be

$$v_f = 9.55 + 0.999\ v_m \qquad (2.1.1)$$

where v_f = fastest-mile speed in miles per hour and v_m = fastest-minute speed in the same hour as the fastest-mile, in miles per hour. Since the slope is very near unity and the mean difference very near 10, it has been assumed for some time that adding 10 mph to the fastest-minute would give an approximation to the fastest-mile". It is this relation which - in the absence of other information - has been used in this report.

While the writers are not certain that Eq. 2.1.1 provides a correct relation between v_f and v_m, they note that it results in estimates of v_f that are conservative from a structural safety point of view.

2.2 MEASURED AND ESTIMATED WIND SPEEDS

With relatively few exceptions the wind speed data used in this report were obtained by measurement. However, at the locations and dates noted below, the extreme annual speeds represent values estimated by the station operator, rather than measured values.

Birmingham, AL	(1973)
Tucson, AZ	(1967)
Sacramento, CA	(1967)
San Diego, CA	(1969)
Denver, CO	(1953)
Moline, IL	(1963)
Des Moines, IA	(1960)
Nantucket, MA	(1966)
Detroit, MI	(1957)
Grand Rapids, MI	(1964)
Jackson, MS	(1966)
Columbia, MO	(1969)
Kansas City, MO	(1971)
Springfield, MO	(1965 & 1971)
Billings, MT	(1959)
Fargo, ND	(1959 &1968)
Albany, NY	(1961)
Rochester, NY	(1958)
Syracuse, NY	(1974)
Cape Hatteras, NC	(1933, 1944 & 1948)
Tulsa, OK	(1959 and 1961)
Portland, OR	(1962)
Roseburg, OR	(1962)
Harrisburg, PA	(1952)
Rapid City, SD	(1962)

Nashville, TN	(1963 & 1972)
Abilene, TX	(1971)
Amarillo, TX	(1972)
Brownsville, TX	(1963)
Corpus Christi, TX	(1955, 1961 & 1970)
Port Arthur, TX	(1972)
Salt Lake City, UT	(1968)
Burlington, VT	(1968)
Lynchburg, VA	(1962 & 1967)

2.3 ROUGHNESS CONDITIONS AT AIRPORT STATIONS

In an attempt to ensure that the terrain roughness conditions are uniform among all the sets of data being analyzed, only airport stations have been considered herein. In principle, it may be assumed that at such stations open exposure conditions prevail. Nevertheless the mere fact that wind speed measurements are taken at an airport station does not necessarily ensure that the wind climatological conditions reflected by these measurements are identical, from the standpoint of the terrain exposure, to those prevailing at a different airport. For example, it is noted in Reference 2 that the estimated 50-year wind at Chicago Midway Airport is about 15 mph less than at the Chicago O'Hare airport. The probable reason for this difference is that the terrain around the Chicago Midway Airport is relatively heavily built-up. Similar considerations might explain to some extent the difference between the estimated 50-year winds at the Washington National Airport and the Baltimore-Washington International Airport, which are estimated in this report to be 66 mph and 75 mph respectively. Thus, in interpreting airport data for the purpose of developing wind maps, it is appropriate to take into account the possibility that, at the airport of concern, the terrain exposure conditions might differ somewhat from those defined as "open" (e.g., in Reference 3).

2.4 VARIATION OF WIND SPEED WITH HEIGHT ABOVE GROUND

To ensure the micrometeorological homogeneity of the data at any given station it is necessary to reduce all the wind speeds recorded at that station to a common elevation. The elevation chosen for this purpose is 10m above ground.

The mean wind profile near the ground in homogeneous terrain is given by the well-known logarithmic law, which may be written in the form:

$$U(z) = \frac{\ln \frac{z}{z_o}}{\ln \frac{10}{z_o}} U(10) \qquad (2.4.1)$$

where z = height above ground and z_o = roughness length, both expressed in meters. In open terrain, z_o may vary from, say, 0.03m to 0.10m. In this report the reduction of the data to an elevation of 10m is based on the assumption z_o = 0.05m. It can be verified that the errors inherent in the assumption z_o = 0.05m -- when in fact the values z_o = 0.03m or z_o = 0.10m were correct -- are small (of the order of 1% or 2%).

An approximation to Eq. 2.4.1 is given by the power law

$$U(z) = (\frac{z}{10})^{\alpha} U(10) \qquad (2.4.2)$$

where, for open terrain conditions, it is generally assumed α = 1/7 (3). It is noted that Eq. 2.4.1, and therefore its approximate equivalent given by Eq. 2.4.2, is valid for mean wind speeds averaged over a relatively long time interval, e.g., one hour. The question thus arises of expressing the variation with height of the fastest-mile wind speed, which is averaged over a relatively short time (30 to 90s or so).

To obtain an approximate expression for the fastest-mile wind profile, note that it may be assumed, approximately,

$$\frac{U_{pk} - U_{fm}}{U_{pk} - U} = \frac{1}{2} \qquad (2.4.3)$$

where U_{pk} = peak wind speed, U_{fm} = fastest-mile speed, and U = hourly mean speed (see, e.g., Reference 4, p. 62). The expression for U_{pk} can, in open terrain, be written as

$$U_{pk}(z) = U(z) + 3\,\overline{u'^2}^{1/2} \qquad (2.4.4)$$

where $\overline{u'^2}^{1/2}$ = r.m.s of longitudinal velocity fluctuations, and

$$\overline{u'^2}^{1/2} = \frac{U(10)}{\ln \frac{10}{z_o}} \qquad (2.4.5)$$

where z_o is expressed in meters (see Reference 4, pp. 45 and 54).

It can be verified by using Equations 2.4.1, 2.4.3, 2.4.4 and 2.4.5 that, within the anenometer elevation range of interest in this report, it is possible to write approximately

$$\frac{U_{fm}(10)}{U_{fm}(z)} = \frac{U(10)}{U(z)} \left(1 + \frac{z-10}{10} 0.02\right) \qquad (2.4.6)$$

where z is expressed in meters. The errors inherent in Equation 2.4.6 are of the order of -1 to 3%, the higher errors being on the conservative side (i.e., yielding slightly higher fastest-mile values at 10m above ground than would be obtained by a more "exact" expression). Eq. 2.4.6 has been employed to obtain the corrected speeds at 10m above ground in this report.

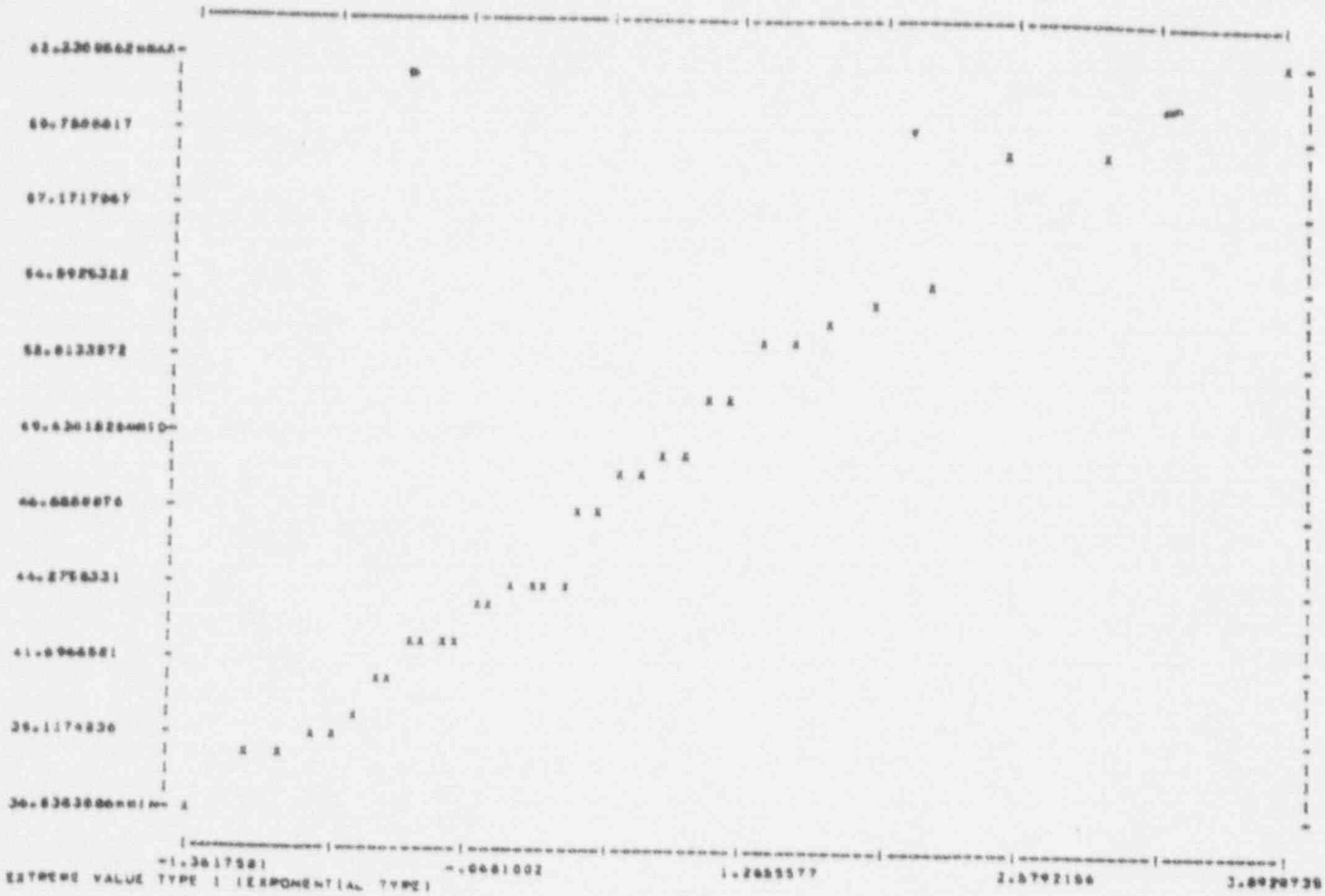

3. STATISTICAL ANALYSIS

3.1 OBJECTIVE OF STATISTICAL PROCEDURE

Probabilistic considerations, as well as available empirical evidence suggest that the asymptotic probability distributions of the largest values with unlimited upper tail are an appropriate model for the behavior of the largest yearly wind speed. There are two such distributions, known as the Type I and Type II distributions of the largest values, whose cumulative distributions functions, $F_I(v)$ and $F_{II}(v)$, respectively, are of the form

$$F_I(v) = \exp\left[-\exp\left(-\frac{v-\mu}{\sigma}\right)\right]; -\infty < v < \infty;$$

$$-\infty < \mu < \infty;\ 0 < \sigma < \infty$$

$$\text{and } F_{II}(v) = \exp\left[-\left(\frac{v-\mu}{\sigma}\right)^{-\gamma}\right];\ \mu < v < \infty;$$

$$-\infty < \mu < \infty;\ 0 < \sigma < \infty;\ \gamma > 0 \qquad (3.1.2)$$

in which μ, σ, and γ are location, scale, and tail length parameters, respectively. Actually, the Type I distribution may be shown to be a Type II distribution with $\gamma = \infty$ (see Reference 4, p. 422); however, it is convenient to refer to it separately.

The data were analyzed using -- with minor modifications -- a computer program listed in Reference 5. For convenience, the main features of the procedure used in the analysis of the data are summarized in this section.

The procedure consists of three distinct stages. In the first stage the value of γ (Eq. 3.1.2) is determined which yields the closest fit to the observed data set (recall that $\gamma = \infty$ corresponds to an extreme value type I distribution). The "closest fit" criterion used in this stage is the so-called maximum probability plot correlation coefficient criterion. The probability plot correlation coefficient is defined as

$$r_D = \mathrm{Corr}(X,M) = \frac{\Sigma(X_i - \overline{X})\,[M_i(D) - \overline{M(D)}]}{\{\Sigma(X_i - \overline{X})^2\ \Sigma[M_i(D) - \overline{M(D)}]^2\}^{1/2}} \qquad (3.1.3)$$

in which $\overline{X} = \Sigma X_i/n$; $\overline{M(D)} = \Sigma M_i(D)/n$; n=sample size; and D = probability distribution tested. The quantities X_i are obtained by a rearrangement of the data set: X_1 is the smallest; X_2 the second smallest; and X_i the ith smallest of the observations in the set. The quantities $M_i(D)$ are obtained as follows. Given a random variable X with probability distribution D and given an integer sample size n, it is possible from probabilistic considerations to derive mathematically the distributions of the smallest, second smallest, and generally the ith smallest values of X in a sample of size n. There are various quantities that can be utilized to measure the location of the distribution of the ith smallest value X_i (e.g., the mean, the median, or the mode). It is convenient to use the median as a measure of location in Eq. 3.1.3 -- these medians of the distribution of the ith smallest value being denoted by $M_i(D)$.

If the data set was generated by the distribution D, then aside from a location and scale factor, X_i will be approximately equal to $M_i(D)$ for all i, and so the plot of X_i versus $M_i(D)$ [referred to as probability plot] will be approximately linear. This linearity will, in turn, result in a near unity value in r_D. Thus, the better the fit of the distribution, D, to the data, the closer r_D will be to unity.

The procedure just described makes use of 46 extreme value Type II distributions defined by various values of γ from 1-25 in steps of 1, from 25-50 in steps of 5, from 50-100 in steps of 10, from 100-500 in steps of 50, from 500-1,000 in steps of 250, and $\gamma = \infty$. For any given data set, 46 probability plot correlation coefficients are computed corresponding to these distributions, and the distribution with the maximum probability plot correlation coefficient is chosen as the one which best fits the data (see, for example, computer output for Dallas, Texas, Section 4). The final result from this first stage is a value, γ_{opt}, of γ corresponding to the estimated best fitting distribution.

The second stage in the procedure consists of estimating the location and scale parameters, μ and σ, respectively, in Eqs. 3.1.1 and 3.1.2 for the observed data set and for the determined optimal value, γ_{opt}, as determined in stage 1. Estimates of the location and scale follow directly from the basic probability plot approach. If a least-squares line is fit to the probability plot corresponding to γ_{opt}, then the computed intercept and slope of the fitted line serve as estimates for the unknown location and scale parameters, μ and σ. In terms of the X_i and $M_i(D)$, these estimated location and scale values, $\hat{\mu}$ and $\hat{\sigma}$, are as follows:

$$\hat{\sigma} = \frac{\Sigma(X_i - \overline{X})[M_i(D) - \overline{M(D)}]}{\Sigma[M_i(D) - M(D)]^2} \qquad (3.1.4)$$

$$\hat{\mu} = \overline{X} - \hat{\sigma}\,\overline{M(D)} \qquad (3.1.5)$$

The third and final stage in the procedure determines the predicted wind speed v_N, for various intervals N of interest. The estimate for v_N is

$$v_N = \hat{\mu} + \hat{\sigma} G_{X_{\gamma_{opt}}} (1 - \frac{1}{N}) \qquad (3.1.6)$$

in which γ_{opt} = the optimal value of γ (as determined in stage 1); $\hat{\mu}$ and $\hat{\sigma}$ are the estimates of the location and scale parameters, μ and σ in Eqs. 3.1.1 and 3.1.2 (as determined in stage 2); and $G_{X\gamma_{opt}}(p)$ = the percentage point function of the best fitting extreme value distribution. If $\gamma_{opt} \neq \infty$ (i.e., if a member of the extreme value type II family provides the best fit), then

$$G_{X_{\gamma opt}}(p) = (-\ln p)^{-1/\gamma} \qquad (3.1.7)$$

If $\gamma_{opt} = \infty$ (i.e., if the extreme value type I distribution provides the best fit), then

$$G_{X_{\gamma opt}}(p) = -\ln(-\ln p) \qquad (3.1.8)$$

In effect, the procedure described in this section is an automated equivalent of probability paper plotting in which 46 types of probability paper, corresponding to 46 extreme value distributions, would be used and in which fitting would be carried out on the basis of the least-squares method, rather than by eye.

3.2 PROBABILITY PLOTS

A majority of the Type I probability plots generated by the computer from the data taken at the 129 stations fit a straight line reasonably well (see, e.g., plot included in computer output for Ely, Nevada, Section 4). However, in a number of cases the fit was relatively poor. A discussion of various reasons leading to a poor fit is presented in Section 3.5. To provide an idea of various types of deviations from a Type I distribution, probability plots were included in Section 4 for the following stations: Indianapolis, Indiana; Des Moines, Iowa; Topeka, Kansas; Wichita, Kansas; Boston, Massachusetts; Nantucket, Massachusetts; Detroit, Michigan; Grand Rapids, Michigan; Minneapolis, Minnesota; Missoula, Montana; Omaha, Nebraska; Valentine, Nebraska; Ely, Nevada; Albuquerque, New Mexico; Albany, New York; Abilene, Texas; and North Head, Washington.

3.3 ESTIMATION OF SAMPLING ERRORS

As indicated in Section 1, the computer output of Section 7 includes estimates of the standard deviation of the sampling errors, i.e., errors that are a consequence of the limited size of the data sample from which the Type I distribution parameters are estimated. Two such estimates were used. One estimate is based on the method of moments and has the following expression given by Gumbel in Reference 6 (pp. 10,174 and 228):

$$SD(\hat{v}_N) = \left[\frac{\pi^2}{6} + \frac{1.1396(y-0.5772)}{\sqrt{6}} + 1.1(y-0.5772)^2\right]^{1/2} \frac{\hat{\sigma}}{\sqrt{n}} \qquad (3.3.1)$$

in which $SD(\hat{v}_N)$ = the (estimated) standard deviation the sampling error in the estimation of the N-year wind

$$y = -\ln\left[-\ln\left(1 - \frac{1}{N}\right)\right] \qquad (3.3.2)$$

$\hat{\sigma}$ = the estimated value of the scale parameter; and n = the sample size.

A lower bound for the estimated sampling error is given by the following expression:

$$SD_{CR}(\hat{v}_N) = (0.60793y^{*2} + 0.514y + 1.10866)^{1/2} \frac{\hat{\sigma}}{\sqrt{n}} \quad , \qquad (3.3.3)$$

where the notations are the same as in Equation 3.3.1. Equation 3.3.3 is commonly referred to as the Cramer-Rao lower bound (7).

3.4 SUMMARY OF RESULTS

The results of the analysis are summarized in Table 3.4.1, in which the following notations are used:

n = sample size

$\overline{X}$ = sample mean

s = sample standard deviation

v_{max} = sample maximum

γ_{opt} = value of optimal tail length parameter (see section 3.1)

$\hat{v}_n$ = estimated extreme wind corresponding to a n-year return period, based on Type I distribution

ppcc = probability plot correlation coefficient (see Section 3.1) for Type I distribution

$\hat{v}_{50}$ = estimated 50-year wind speed

$SD(\hat{v}_{50})$ = estimated standard deviation of sampling error for 50-year wind speed.

3.5 TYPE I VERSUS TYPE II DISTRIBUTION

Of the 129 stations listed in Table 3.4.1, 15 stations [marked with the superscript (c) in Table 3.4.1 and listed in Appendix 1] have been noted to have largest yearly speed records that may not provide a reliable basis for predicting extreme winds. The remaining 114 stations may be divided into three categories characterized by the value of the optimal tail length parameter γ_{opt}, as shown in Table 3.5.1.

Table 3.5.1 Classification of Stations According to Value of γ_{opt}

Category	Range of γ_{opt}	Number of Stations	Percentage
I	$13 \leq \gamma_{opt} < \infty$	89	78%
II	$7 \leq \gamma_{opt} < 13$	11	10%
III	$2 \leq \gamma_{opt} < 7$	14	12%

The sample size for the stations of Table 3.5.1 varies between n=10 and n=45.

It is noted that the percentages of Table 3.5.1 are in qualitative agreement with those found from the analysis reported in Reference 8, in which all sample sizes were n = 37. This tends to confirm the hypothesis advanced in Reference 8 to the effect that, for stations in well-behaved wind climates, the best fit of a Type II (rather than Type I) distribution to a set of extreme wind data might be attributed to a sampling error in the estimation of the tail length parameter. This hypothesis does not exclude the possibility that stations exist for which a Type II distribution might provide an appropriate description of the wind climate; however, according to the results of both Reference 8 and Table 3.5.1, the number of such stations, if they exist, is very likely to be small. Thus, it appears justified to assume, as in Reference 8, that the Type I distribution of the largest values provides in general a better description of the wind climate than Type II distributions with small values of the tail length parameter (say, $2 \leq \gamma \leq 12$).

3.6 LARGEST WIND SPEED IN A SAMPLE OF SIZE N AND THE N-YEAR WIND

It is shown in Reference 9 (see also Reference 4, p. 423) that, if a variate X has a Type I distribution, the mode of the largest value in a sample of n values of X is very nearly equal to the value of the variate corresponding to the mean return period n (recall that the mode of a variate X is the value of that variable most likely to occur in any given trial). It can be seen from Table 3.5.1 that, for most sets for which γ_{opt} is large, the ratio $v_{max}/\hat{v}_n$ is indeed close to unity.

OMAHA, NEBRASKA (1936-1977)

THE SAMPLE NUMBER OF OBSERVATIONS	=	42.00
THE SAMPLE MEAN	=	55.00
THE SAMPLE STANDARD DEVIATION	=	10.67
THE SAMPLE MINIMUM	=	42.69
THE SAMPLE MAXIMUM	=	104.00

DATE	ANEMOMETER ELEVATION(FT)	FASTEST MILE WIND SPEED AND DIRECTION (RECORDED AT ANEMOMETER ELEVATION)	CALCULATED FASTEST MILE WIND SPEED AT 10M ABOVE GROUND (CORRECTED SPEED)
07/19/36	44.	109. N	104.
03/23/37	44.	73. E	70.
08/07/38	44.	63. SW	60.
10/04/39	44.	59. SW	56.
05/14/40	44.	50. NW	48.
07/10/41	68.	63. NW	57.
06/19/42	68.	72. N	65.
08/11/43	68.	55. SW	49.
08/01/44	68.	66. N	59.
07/27/45	68.	54. N	48.
04/03/46	68.	49. W	44.
07/12/47	68.	65. NE	58.
04/03/48	68.	49. S	44.
10/10/49	68.	59. S	53.
03/07/50	68.	73. NW	66.
11/05/51	68.	56. NW	50.
08/19/52	68.	59. W	53.
05/10/53	68.	59. SW	53.
04/20/54	68.	54. NW	48.
01/28/55	74.	49. NW	44.
07/07/56	74.	57. NW	51.
05/16/57	74.	58. E	52.
07/08/58	74.	54. S	48.
05/20/59	74.	65. W	58.
08/05/60	74.	55. N	49.
04/15/61	74.	50. NW	44.
05/07/62	74.	56. NW	50.
12/08/63	20.	49. NW	54.
05/25/64	20.	63. NW	69.
01/31/65	20.	45. NW	49.
03/23/66	20.	50. N	55.
06/04/67	20.	56. N	61.
05/15/68	20.	65. NW	71.
01/05/69	20.	39. NW	43.
02/02/70	20.	47. NW	51.
06/18/71	20.	56. NW	61.
01/24/72	20.	47. NW	51.
05/09/73	20.	50. N	55.

08/16/74	20.	44. NE	48.
11/20/75	20.	44. NW	48.
04/16/76	20.	58. S	63.
01/27/77	20.	45. NW	49.

RETURN PERIOD (IN YEARS)	PREDICTED EXTREME WIND BASED ON OPTIMAL EXTREME VALUE TYPE 2. DISTRIBUTION (GAMMA = 3.00000)	PREDICTED EXTREME WIND BASED ON EXTREME VALUE TYPE 1 DISTRIBUTION	ESTIMATED STAN. DEV. SAMPL. ERROR CRAMER-RAO	ESTIMATED STAN. DEV. SAMPL. ERROR METH. OF MOM.
2.0	51.98	53.41	1.51	1.51
3.0	55.54	57.64	1.85	1.92
4.0	58.18	60.67	2.11	2.27
5.0	60.34	62.76	2.31	2.55
6.0	62.19	64.43	2.48	2.78
7.0	63.82	65.81	2.63	2.98
8.0	65.29	67.00	2.76	3.15
9.0	66.64	68.03	2.87	3.30
10.0	67.88	68.95	2.97	3.44
20.0	77.13	74.89	3.63	4.34
30.0	83.55	78.31	4.02	4.87
40.0	88.63	80.72	4.30	5.25
42.0	89.54	81.12	4.35	5.32
50.0	92.92	82.58	4.52	5.55
60.0	96.66	84.09	4.69	5.79
70.0	100.00	85.38	4.84	5.99
80.0	103.04	86.49	4.97	6.17
90.0	105.83	87.46	5.09	6.32
100.0	108.41	88.34	5.19	6.46
200.0	127.89	94.08	5.87	7.38
300.0	141.54	97.43	6.26	7.92
400.0	152.40	99.80	6.55	8.30
500.0	161.57	101.65	6.77	8.60
600.0	169.59	103.15	6.95	8.84
700.0	176.75	104.42	7.10	9.04
800.0	183.26	105.53	7.23	9.22
900.0	189.25	106.50	7.35	9.38
1000.0	194.81	107.37	7.45	9.52
2000.0	236.69	113.09	8.13	10.44
3000.0	266.06	116.43	8.54	10.99
4000.0	289.43	118.81	8.82	11.37
5000.0	309.18	120.65	9.04	11.67
6000.0	326.44	122.15	9.22	11.91
7000.0	341.87	123.43	9.37	12.12
8000.0	355.90	124.53	9.51	12.30
9000.0	368.79	125.50	9.62	12.46
10000.0	380.78	126.37	9.73	12.60
50000.0	627.14	139.65	11.33	14.75
100000.0	781.37	145.36	12.02	15.68
500000.0	1312.77	158.65	13.62	17.84
1000000.0	1645.20	164.37	14.31	18.77

ATTACHMENT #2

RECORD OF TELEPHONE COMMUNICATION

M. R. NO. ________ FILE NO. PED-FC-91-2059

DATE: 4/24/91 TIME: 1:30PM TELEPHONE NO. (301) 975-6076

PARTY CALLING: Mike Elzway (Name) OPPD (Company)

PARTY ANSWERING: Emil Simiu (Name) National Bureau of Standards (Company)

SUBJECT: NBS Building Science Series 118, Extreme Wind Speeds at 129 Stations in the Contiguous United States

---

TELECON SUMMARY (Including Decisions and Commitments):

I asked Mr. Simiu for the latest NBS Building Scien.e Series 118. Mr. Simiu stated that the latest was issued in March 1979. He also stated that this Series will be reissued within one year from now. I told Mr. Simiu that the Series covers extreme wind speeds from only 1936 to 1977 for the Omaha area, then I asked if additional wind data is available for Omaha. Mr. Simiu stated he has wind data for Omaha up to 1986, as follows:

Year	Calculated Fastest Mile Wind Speed at 10m above ground (corrected speed)
1978	45
1979	40
1980	50
1981	40
1982	56
1983	44
1984	43
1985	39
1986	40

Mr. Simiu stated that this additional data makes the return period greater for most wind speeds tabulated on page 162 of the NBS Series 118.

ACTION REQUIRED:

DISTRIBUTION:

ATTACHMENT #3

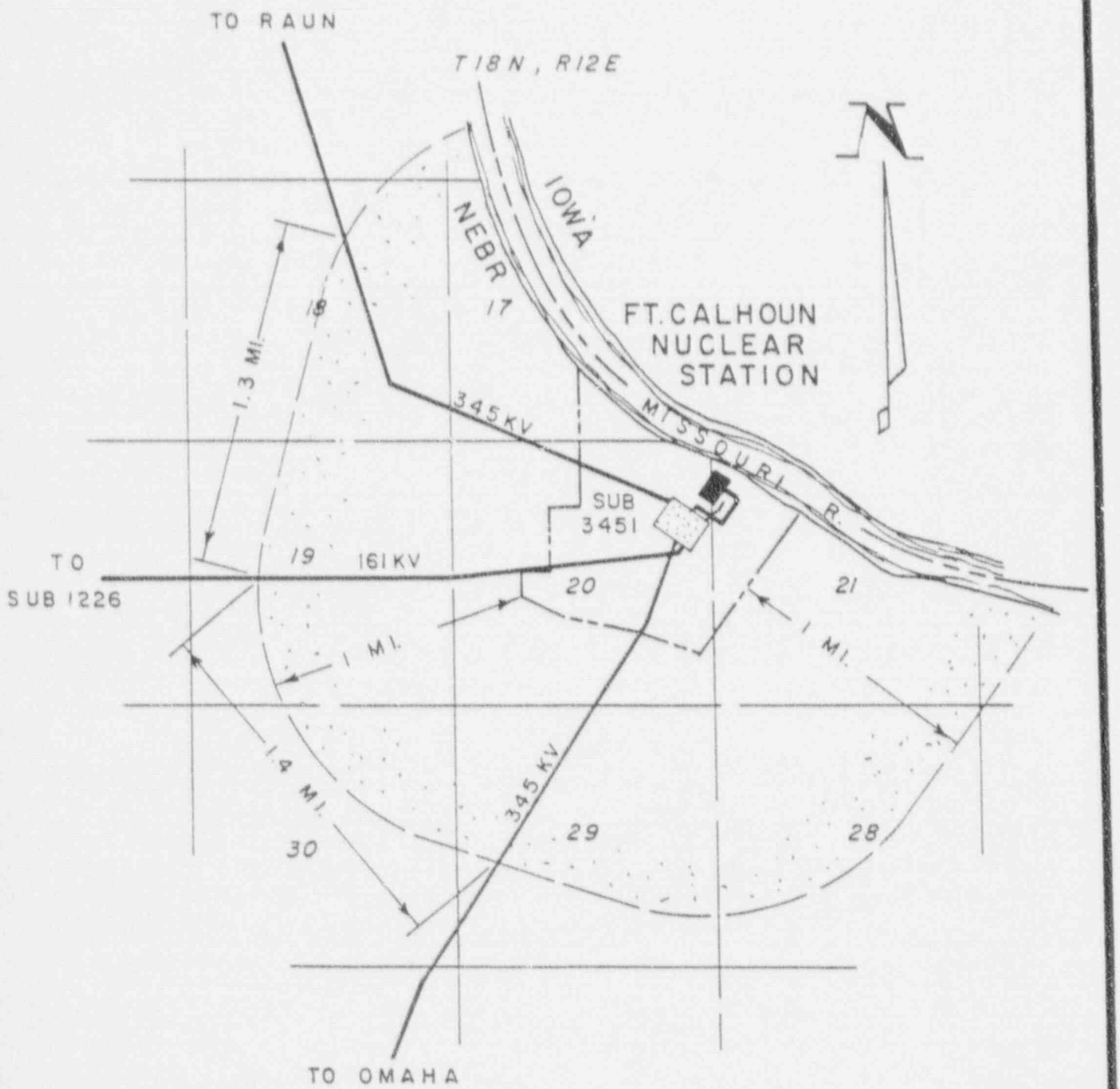

SCALE	1" = 3000'	
DRAFT	11-14-88	
CHECK		
PROJ. ENG.		
APPD.		
DEPT.	TRANS.	

TRANSMISSION LINES AT FT. CALHOUN STATION

OMAHA PUBLIC POWER DISTRICT

A 934

ATTACHMENT #4

Evaluation for the Effect of CEDM Mechanical Seal Failure on Fort Calhoun Station Blackout event (EA-89-018)

The analysis is based on an extremely conservative value of 20% of the maximum possible CEDM leakage for the seal housing area. Actual leakage by experiment (CRDM (CEDM) Mechanical Seal Test, October 1989) was calculated to be 0.1 gpm. The use of the larger leakage rate in the analysis was to ensure a conservative result. Analysis was performed using the best estimate Combustion Engineering Transient Simulation Code (CENTS). Key input assumptions/parameters are shown below. The code has a quality assured base deck for Fort Calhoun for all components in the NSSS and secondary system model.

Assumed:
1) 110 gpm leakage - RCP pumps and unknown. (constant throughout event)
2) Letdown rampdown from 36 gpm to zero over 300 sec (5 minutes).
3) RV Volume to cover core = 11.2 ft from center of bottom core support plate.

Sequence of Events

Time(Seconds)	Event/Parameters
0.0	Initiation of Station Blackout CEDM Leakage = 0 RCS Flow = 20,066 lbm/sec RCS Nodal Height = 19.2 ft RV Head Nodal Height = 9.4 ft RCS average temperature = 578^{0}F RCS pressure = 2,110 psi Pressurizer Nodal Height = 13.3 ft RCP seal leak rate of 25 gpm/pump = 100 gpm Unknown sources leakage = 10 gpm
3.0	Reactor trip on low flow CEDM Leakage = 0 RCS Flow = 13,831 lbm/sec RCS Nodal Height = 19.2 ft RV Head Nodal Height = 9.4 ft RCS average temperature = 580^{0}F RCS Pressure = 2,103 psi Pressurizer Nodal Height = 13.2 ft
25.0	Feed Water is ramped down to zero. CEDM Leakage = 0 RCS Nodal Height = 19.2 ft RV Head Nodal Height = 9.4 ft RCS average temperature = 573^{0}F RCS Pressure = 1,995 psi Pressurizer Nodal Height = 12.0 ft

40.0	SG safeties open (beyond this point they cycle). CEDM Leakage = 0 RCS Nodal Height = 19.2 ft RV Head Nodal Height = 9.4 ft RCS average temperature = 571^{0}F RCS Pressure = 1,976 psi Pressurizer Nodal Height = 11.2 ft
180.0	Auxiliary Feed is delivered at a rate of 260 gpm. CEDM Leakage = 0 RCS Nodal Height = 19.2 ft RV Head Nodal Height = 9.4 ft RCS average temperature = 570^{0}F RCS Pressure = 1,914 psi Pressurizer Nodal Height = 9.2 ft
300.0	Letdown flow is ramped down to zero. CEDM Leakage = 0 RCS Nodal Height = 19.2 ft RV Head Nodal Height = 9.4 ft RCS average temperature = 570^{0}F RCS Pressure = 1,874 psi Pressurizer Nodal Height = 8.0 ft
1,340.0	SIAS is generated. CEDM Leakage = 0 RCS Nodal Height = 19.2 ft RV Head Nodal Height = 9.4 ft RCS average temperature = 564^{0}F RCS Pressure = 1,606 psi Pressurizer Nodal Height = 2.0 ft
2,340.0	Steam bubble formed in RV Head. CEDM Leak initiated. CEDM Maximum Leakage = 10.3 lbm/sec (1574 gpm)* RCS Nodal Height = 19.2 ft RV Head Nodal Height = 8.4 ft (RV upper head void 1 foot) RCS average temperature = 556^{0}F RCS Pressure = 1,272 psi Pressurizer Nodal Height = 1.4 ft

* initial leak rate will decrease during remainder of the event.

14,400.0	Four hours into SBO event. CEDM Leakage < 10.3 lbm/sec RCS Nodal Height = 16.9 ft (RV level is below nozzles) RCS average temperature = 530^{0}F RCS Pressure = 882 psi
20,520.0	Five hours 42 minutes into SBO event. Core uncovery CEDM Leakage < 10.3 lbm/sec RCS Nodal Height = 11.2 ft RCS average temperature = 550^{0}F RCS Pressure = 1,046 psi

Calculation FC 05695 verifies by use of a mass/energy balance the SBO event is bounded by the containment conditions present for the LOCA/MSLB events.

Key nodal volumes of the NSSS and reactor vessel are shown in the enclosed sketches.

FORT CALHOUN STATION

APPROXIMATE RCS VOLUMES
(All Volumes in Ft^3)

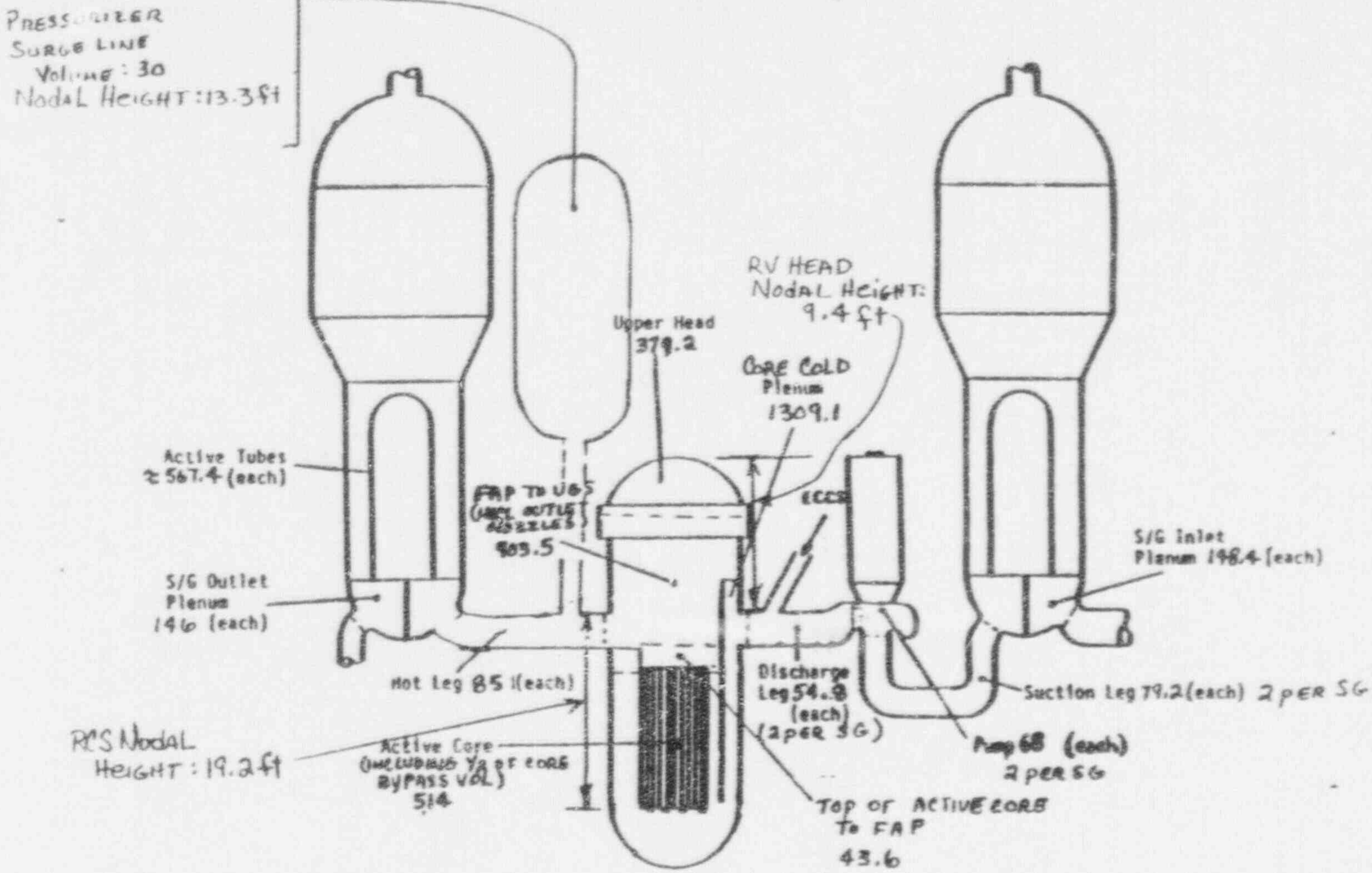

TOTAL HFP RCS WATER VOLUME = 6381.1 ft^3

(REF: TDB-III.3.B-1 THRU E-1)

FCS Volume at Beginning of Core Uncovery

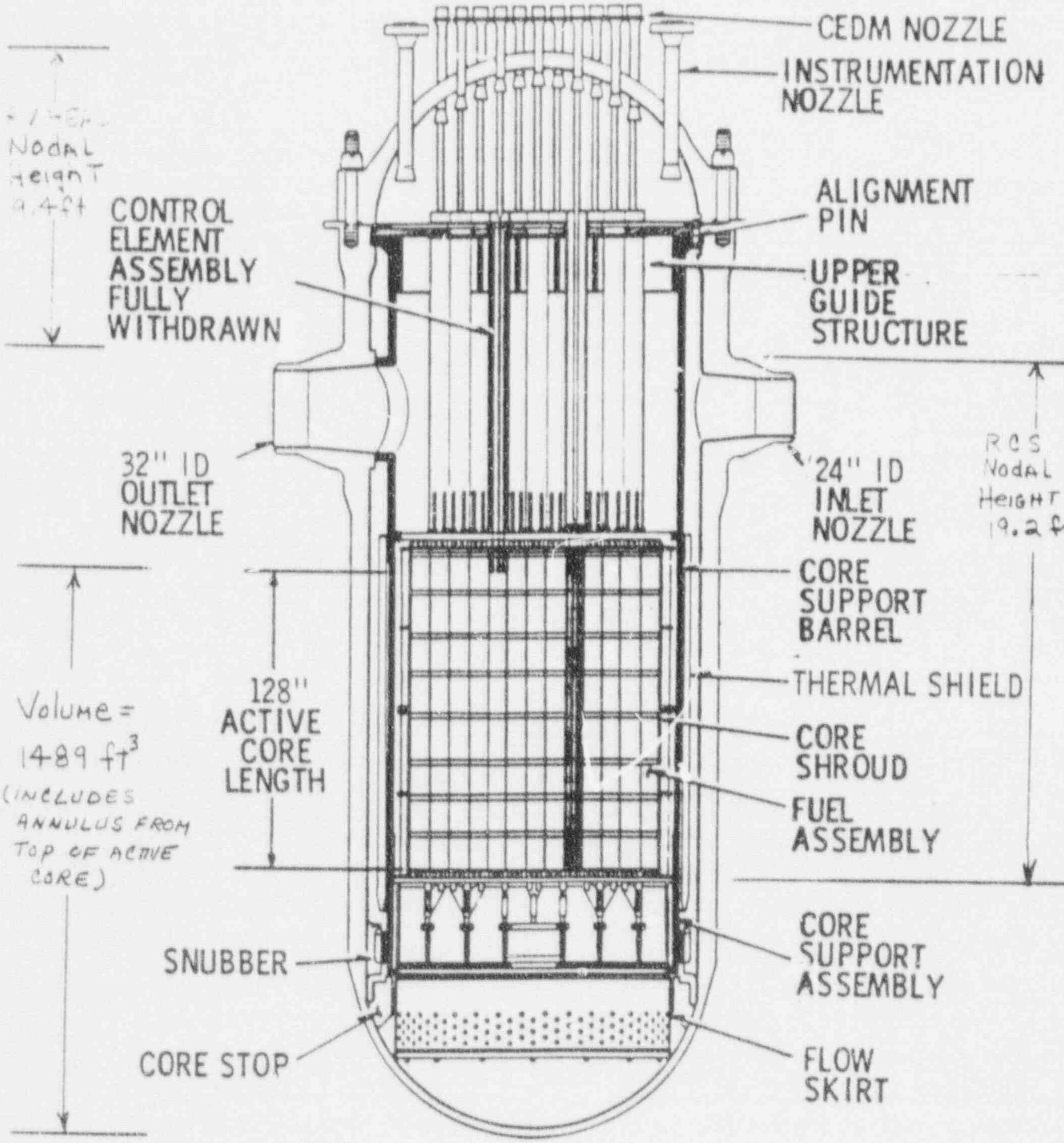

Reactor Arrangement	Omaha Public Power District Fort Calhoun Station-Unit No. 1	Figure 1-2A

JUNE, 1970